Protein Science (2000), *9*:907–915. Cambridge University Press. Printed in the USA.

Alternate modes of binding in two crystal structures of alkaline phosphatase-inhibitor complexes

KATHLEEN M. HOLTZ,[1] BOGUSLAW STEC,[2] JASON K. MYERS,[3] STEPHEN M. ANTONELLI,[3] THEODORE S. WIDLANSKI,[3] AND EVAN R. KANTROWITZ[1]

[1]Department of Chemistry, Boston College, Chestnut Hill, Massachusetts 02467
[2]Department of Chemistry, Rice University, Houston, Texas 77005
[3]Department of Chemistry, Indiana University, Bloomington, Indiana 47405

(RECEIVED March 3, 1999; FINAL REVISION February 21, 2000; ACCEPTED March 23, 2000)

Abstract

Two high resolution crystal structures of *Escherichia coli* alkaline phosphatase (AP) in the presence of phosphonate inhibitors are reported. The phosphonate compounds, phosphonoacetic acid (PAA) and mercaptomethylphosphonic acid (MMP), bind competitively to AP with dissociation constants of 5.5 and 0.6 mM, respectively. The structures of the complexes of AP with PAA and MMP were refined at high resolution to crystallographic *R*-values of 19.0 and 17.5%, respectively. Refinement of the AP-inhibitor complexes was carried out using X-PLOR. The final round of refinement was done using SHELXL-97. Crystallographic analyses of the inhibitor complexes reveal different binding modes for the two phosphonate compounds. The significant difference in binding constants can be attributed to these alternative binding modes observed in the high resolution X-ray structures. The phosphinyl group of PAA coordinates to the active site zinc ions in a manner similar to the competitive inhibitor and product inorganic phosphate. In contrast, MMP binds with its phosphonate moiety directed toward solvent. Both enzyme-inhibitor complexes exhibit close contacts, one of which has the chemical and geometrical potential to be considered an unconventional hydrogen bond of the type C-H···X.

Keywords: inhibitors; phosphatase; phosphonates; phosphonic acid; X-ray crystallography

Alkaline phosphatase from *Escherichia coli* (EC 3.1.3.1, AP) is a homodimeric, metalloenzyme catalyzing the nonspecific hydrolysis of phosphate monoesters. The enzymatic reaction proceeds through a phosphoseryl intermediate to produce inorganic phosphate and an alcohol. AP has been extensively studied and is a model system for understanding enzymatic catalysis involving metal ions. Each active site of AP contains one magnesium ion (Mg) and two zinc ions (Zn_1 and Zn_2) that roughly trace a triangle. Almost identical catalytic triads can be found in two related phosphoesterases, phospholipase C from *Bacillus cereus* (Hough et al., 1989) and P1 nuclease from *Penicillium citrinum* (Volbeda et al., 1991). The metal binding sites of these enzymes have ligands with side chains of similar chemical identity and arrangement (Coleman, 1992).

The proposed two-metal ion-assisted catalytic mechanism of AP is based on the high resolution X-ray crystal structure of the wild-type enzyme in a complex with inorganic phosphate (Kim & Wyckoff, 1991). The structure of the phosphate-free enzyme has been determined to 2.8 Å resolution (Sowadski et al., 1983, 1985). Additional X-ray structures of AP in recent studies have focused on capturing different steps in the catalytic cycle of AP. The phosphoseryl catalytic intermediate has been captured in a crystal structure of the H331Q mutant determined to 2.3 Å (Murphy et al., 1997). The X-ray crystal structure of the AP-vanadate (VO_3^-) complex determined to 1.9 Å serves as a model for the proposed transition state in the formation and decomposition of the covalent phosphoseryl intermediate (Holtz et al., 1999). In this study, complexes of the enzyme with competitive phosphonate inhibitors are determined by X-ray crystallography. These structures are the first enzyme-phosphonate complexes of AP determined by X-ray crystallography. Although intended to provide structural models for the noncovalent enzyme-substrate complex, the only catalytic step of AP without a structural representation, the structures with the phosphonates bound in the active site provide valuable information on alkaline phosphatase inhibition and sheds light on the limitations of phosphonates as phosphatase inhibitors.

The inhibition of AP presents a unique challenge since the active site pocket is characteristically shallow. Inorganic phosphate, one of the tightest binding inhibitors of *E. coli* AP, essentially fills the entire volume of the active site (Kim & Wyckoff, 1991). While this feature allows the enzyme to hydrolyze a wide variety of substrates

Reprint requests to: Evan R. Kantrowitz, Boston College, Department of Chemistry, Merkert Chemistry Center, Chestnut Hill, Massachusetts 02467; e-mail: evan.kantrowitz@bc.edu.

Abbreviations: AP, alkaline phosphatase; PAA, phosphonoacetic acid; MMP, mercaptomethylphosphonic acid; R166A, alkaline phosphatase in which arginine at position 166 is replaced with an alanine.

close to the same rate regardless of the nature of the R group, it does not afford many opportunities for enzyme-ligand interactions. For this reason, phosphonates (Engel, 1977; Holden et al., 1987; Lejczak et al., 1989; Bartlett et al., 1990; Kim & Lipscomb, 1990; Morgan et al., 1991), widely used as nonhydrolyzable analogs of the parent phosphate monoesters, are generally not very strong inhibitors of the enzyme. In fact, small inorganic ions that include inorganic phosphate (10 μM), vanadate (2 μM), and periodate (0.05 μM) (Reid & Wilson, 1971; Ohlsson & Wilson, 1974; Lopez et al., 1976) are the most potent inhibitors of AP. Recently reported are a group of new phosphonate inhibitors of metallophosphatases (Myers et al., 1997) that contain pendant groups capable of ligation to active site metals. Even the most poorly binding of these compounds displays enhanced inhibition of metallophosphatases relative to an unsubstituted phosphonate. The inhibitory potency of *o*-mercaptophenylphosphonic acid (0.21 μM), the most potent of these small molecule inhibitors, substantially exceeds that of vanadate and phosphate for bovine intestinal alkaline phosphatase (Myers et al., 1997).

To better understand phosphonate inhibition of AP and its improvement, two of these functionalized phosphonic acid compounds (Fig. 1), phosphonoacetic acid (PAA) and mercaptomethylphosphonate (MMP), have been evaluated kinetically and structurally as inhibitors and potential substrate analogs of *E. coli* alkaline phosphatase. These inhibitors are not the tightest binding phosphonate inhibitors available; however, structural analyses have shed light on the difference in binding affinities of these two inhibitors. Structural analyses have also provided some guidelines for the development of more potent inhibitors of AP and for rationalizing observed binding potencies of the currently available inhibitors.

Results

Inhibition constants for AP in the presence of PAA and MMP

The phosphonate inhibitors PAA and MMP competitively inhibit AP with K_i values of 5.5 ± 0.3 and 0.6 ± 0.1 mM, respectively, under standard assay conditions of 1.0 M Tris pH 8.0. The inhibition constants were calculated from double-reciprocal data. PAA, a modest competitive inhibitor of *E. coli* alkaline phosphatase, binds about nine times more weakly than MMP. The difference in K_i values between PAA and MMP represents ~1.3 kilocalories per mole of binding energy. The only difference between the two phosphonates is the substitution of a carboxylate group in PAA for a thiol in MMP. Both of these groups are Lewis bases and electron donors. Both functional groups are known to form complexes with divalent metal ions and have the potential to form complexes with the zinc ions in the active site of alkaline phosphatase.

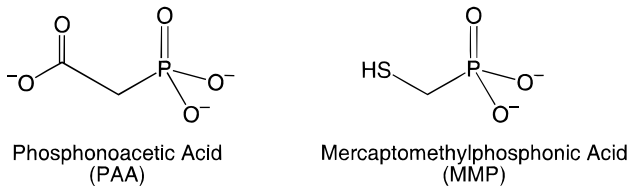

Fig. 1. Structures of AP inhibitors phosphonoacetic acid (PAA) and mercaptomethylphosphonic acid (MMP).

Crystallography

To acquire an explanation for the difference in affinity between PAA and MMP, structural determinations of the enzyme-inhibitor complexes were performed. The refinement statistics for both AP-inhibitor structures are reported in Table 1. Initial refinement of the AP-inhibitor structures was done with X-PLOR (Brünger, 1992), and the final refinement was carried out with SHELXL-97 (Sheldrick & Schneider, 1997). Full matrix refinement using SHELXL-97 (Sheldrick & Schneider, 1997) in the final stage provides coordinate errors (ESD) for interatomic distances in the AP-inhibitor complexes (Table 2). For the AP-PAA complex, the final *R*-factor, calculated at 2.20 Å resolution, is 0.190, and the final free *R*-factor is 0.257. The final model includes 513 water molecules. For the AP-MMP complex, the final *R*-factor, calculated at 2.00 Å resolution, is 0.175, and the final free *R*-factor is 0.229. The final model includes 552 water molecules.

The overall structures of both the AP-PAA and the AP-MMP complexes are remarkably similar to the structure of the wild-type enzyme. The root-mean-square displacement (RMSD) of backbone atoms between the structure of the wild-type enzyme and the structures of the enzyme-inhibitor complexes was determined. These differences are plotted as a function of residue number in Figure 2. The average RMSD between the AP-PAA structure and the wild-type structure is 0.18 and 0.20 Å for the backbone atoms of the A and B chains, respectively. In the case of the AP-MMP structure, the same comparison gives 0.11 Å for the backbone atoms of both the A and B chains.

Refinement of the inhibitors indicates partial occupancies for both PAA and MMP. The occupancy of PAA in each active site of the dimeric enzyme is 70% based on occupancy refinement, while the occupancy of MMP in each active site is 65% based on occupancy refinement. Despite partial occupancies, excellent electron density is observed for the inhibitors bound in the active sites in both the $2F_o - F_c$ and $F_o - F_c$ maps (Fig. 3). The maps indicate reliable structures with accurately positioned residues and inhibi-

Table 1. *Refinement statistics for the structures of the AP-PAA and AP-MMP complexes*

Complex	AP-PAA	AP-MMP
Working *R*-factor		
4σ cutoff	0.151	0.135
All reflections	0.190	0.175
Free *R*-factor[a]		
4σ cutoff	0.212	0.186
All reflections	0.257	0.229
Water molecules[b]	513	552
RMS deviations		
Bond lengths (Å)	0.02	0.02
Bond angles (deg)	1.92	2.00
Improper angles (deg)	1.82	1.89
Dihedral angles (deg)	24.7	24.8

[a]The use of cross-validation with one *R*-free involves the random partitioning of a small percentage (10%) of the observed intensities into a test set *T*. The reflections placed in the test set are not used in the refinement process.

[b]Contour levels in the $(F_o - F_c)$ density maps of 2.5σ were used to identify peaks for water placement.

Table 2. *Enzyme-inhibitor interactions and distances for AP-PAA and AP-MMP complexes*

Complex	Enzyme-inhibitor interaction	Distance (Å) (subunit A/subunit B)[a]
AP-PAA	$Zn_2\cdots O_A$-PO_2-R (phosphonate)[b]	1.59 (0.21)/2.15 (0.15)
	$Zn_1\cdots O_B$-PO_2-R (phosphonate)	1.78 (0.38)/1.71 (0.31)
	$Zn_1\cdots$O-C(O) (carboxyl)	3.20 (0.40)/3.60 (0.34)
	η_1 (Arg166)$\cdots CH_2$ (methylene)	2.72 (0.30)/2.91 (0.15)
	η_2 (Arg166)$\cdots O_C PO_2$R (phosphonate)	2.73 (0.34)/2.72 (0.14)
	Cϵ (His412)$\cdots CH_2$ (methylene)	3.12 (0.14)/3.20 (0.12)
	N (Ser102)$\cdots CH_2$ (methylene)	2.82 (0.14)/3.05 (0.12)
AP-MMP	$Zn_1\cdots$thiol	2.30 (0.05)/2.30 (0.06)
	Oγ (Ser102)$\cdots$thiol	2.65 (0.05)/2.75 (0.06)
	η_1 (Arg166)$\cdots CH_2$ (methylene)	2.73 (0.11)/2.87 (0.10)
	Cϵ (His412)$\cdots CH_2$ (methylene)	3.20 (0.15)/3.20 (0.12)
	N (Ser102)$\cdots CH_2$ (methylene)	3.12 (0.08)/3.11 (0.07)

[a]Estimated standard errors for bond distances are given in parentheses.
[b]Phosphonate oxygen atoms are distinguished by the subscripts A, B, and C.

tors. Analysis of the structural data indicates different modes of binding for PAA and MMP in the active site and some unexpected enzyme-inhibitor interactions as discussed below.

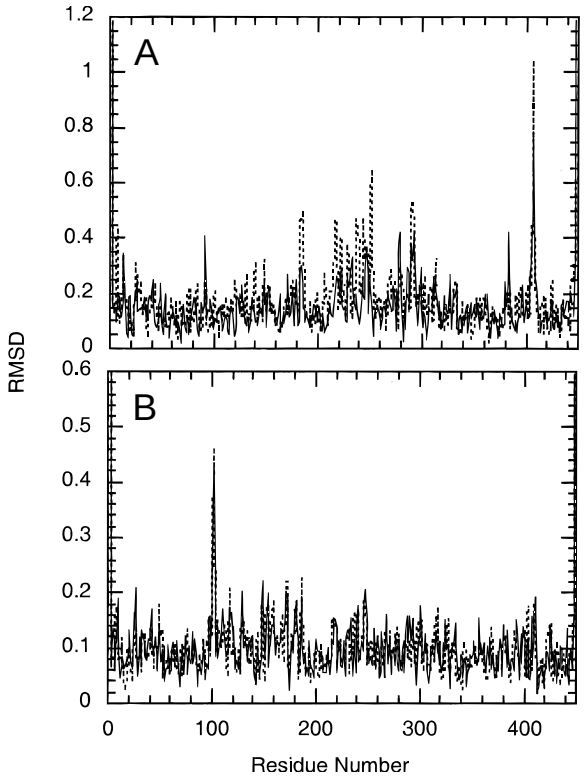

Fig. 2. The plot of the RMSD of the main-chain atoms vs. the residue number between: (**A**) the AP-PAA and the wild-type structures and (**B**) the AP-MMP and the wild-type structures. RMSD of the A chains is represented by the solid line. RMSD of the B chain is represented by the dashed line. Note both structural complexes are highly correlated with the wild-type structure with the average RMSD below 0.2 Å in both comparisons.

Active site of AP with bound PAA

The $2F_o - F_c$ and $F_o - F_c$ maps (Fig. 3A) clearly show PAA bound in the active site cleft of AP. The tetrahedral phosphinyl group of PAA is orientated in a manner similar to inorganic phosphate bound in the active site of the enzyme. The phosphinyl group bridges the two zinc ions using two of its three oxygen atoms to coordinate the metal ions. The third oxygen of the phosphonate portion forms a hydrogen bond to a terminal guanidino nitrogen (η_2) of the Arg166 side chain. In addition, the binding mode of PAA is also characterized by close contacts between the inhibitor and the enzyme. The methylene carbon of PAA is in close proximity to the guanidino nitrogen (η_1) of Arg166 (2.7 Å ± 0.3/2.9 ± 0.2 Å in A/B sites), the imidazole ring carbon (Cϵ) of His412 (3.1 ± 0.3 Å/3.2 ± 0.2 Å in A/B sites), and the backbone amide nitrogen of Ser102 (2.8 ± 0.1 Å/3.1 ± 0.1 Å in the A/B sites). All these interactions are much less than the sum of the van der Waals radii. The importance of these interactions in inhibitor stabilization or destabilization is discussed. It should be noted that in the wild-type structure of the noncovalent enzyme-phosphate complex, a close contact is also observed between the Cϵ carbon of His412 and an oxygen of inorganic phosphate. The terminal carboxylate of PAA is 3.2 and 3.6 Å away from Zn_1 in the A and B sites, respectively. A summary of the relevant AP-PAA interactions and corresponding distances is provided in Table 2.

Active site of AP with bound MMP

The $2F_o - F_c$ and $F_o - F_c$ maps for MMP (Fig. 3B) shows unambiguously the reverse orientation of this phosphonate inhibitor in the active site of AP with the thiol functionality of the inhibitor directed into the active site as a ligand to Zn_1 with an average $Zn\cdots S$ distance of 2.3 Å. Modeling and refinement of the inhibitor in the other orientation, i.e., with the phosphinyl group directed into the active site, results in a very poor fit to the density map and higher thermal vibration coefficients for the sulfur of the inhibitor. In the reverse orientation, the thiol group of the inhibitor is also in a position to form a short hydrogen bond to the Oγ oxygen of the Ser102 nucleophile. The O$\gamma\cdots$S interaction is 2.6

Fig. 3. Stereoview of the final models of the active site of AP with inhibitors bound: (**A**) AP-PAA and (**B**) AP-MMP. The models are superimposed with their respective $2F_o - F_c$ density maps (in yellow) contoured at 1.5σ and omit $F_o - F_c$ density maps (in red) contoured at 3.5σ. Residues are color coded according to formal charge (negative, red; positive, blue; neutral, light blue). Partial phosphate occupancy is also shown in the AP-PAA complex. Some crucial distances in both complexes are also given.

and 2.7 Å in the A and B sites, respectively. The orientation of MMP also places the phosphonate portion of the inhibitor outside of the active site directed out into solution. The phosphinyl oxygen atoms have no direct interactions with the enzyme. Similar to PAA, the methylene carbon of MMP is in close contact to the guanidino nitrogen atom (η_1) of Arg166 (2.7 ± 0.1 Å/2.9 ± 0.1 Å in A/B sites), the imidazole ring carbon (Cϵ) of His412 (3.2 ± 0.2 Å/ 3.2 ± 0.1 Å in the A/B sites), and the backbone amide nitrogen of Ser102 (3.1 ± 0.1 Å/3.1 ± 0.1 Å in the A/B sites). These interactions and the unexpected conformation adopted by MMP are discussed. A summary of the relevant AP-MMP interactions and corresponding distances is provided in Table 2.

Discussion

Reverse binding mode of MMP; implications for stronger inhibition

The reverse binding mode of MMP is unexpected. The structural study with MMP reveals an alternative binding mode for a phosphonate compound in the active site of AP. Crystallography identified the thiol moiety of MMP to be the preferred ligand to zinc rather than the phosphonate group of MMP. The distance between Zn_1 and the thiolate is 2.3 Å in agreement with Zn···S distances found in other metalloproteins (Chakrabarti, 1989). The hydroxyl group of the Ser102 nucleophile forms a short hydrogen bond to the thiol group of MMP. The phosphonate group, however, is completely removed from the catalytic center. Based upon the AP complex with PAA, phosphonate groups have the potential to form at least three very strong salt bridges with active site features of AP. The phosphinyl oxygen atoms can coordinate Zn_1 and Zn_2 and participate in a hydrogen bond with the guanidino side chain of Arg166. The combined enzyme-oxygen interactions that could occur between the phosphonate moiety and the active site zinc ions and Arg166 are forfeited for a direct metal-sulfur interaction and a short S···H···O hydrogen bond. The active site's preference for the thiol group over the phosphonate moiety in MMP may be correlated with its kinetic binding affinity. MMP has a K_i value of 0.6 mM for MMP, approximately ninefold lower than that observed for PAA. Prior to crystallographic analysis, a basis for this difference in inhibitor binding was unknown.

The observed difference in binding affinities reflects the stronger interactions of the thiol group of MMP with the enzyme and suggests a potential role for thiols as more potent inhibitors of

alkaline phosphatases. Although the phosphonate group does not have any direct interactions with active site metals, this functional group may indirectly participate in MMP binding. For example, reasonable concentrations of simple thiols, such as 2-mercaptoethanol, thiophenol, and ethanethiol, do not function as inhibitors of the enzyme, suggesting that the negative charge on the phosphonate is still necessary for binding. The electrostatic surface potential of AP indicates a strongly cationic active site. Attractive forces between the negatively-charged phosphonate group of the inhibitor may be important in directing the molecule into the positively charged active site pocket. Once in the vicinity of the active site, MMP adopts the lowest energy orientation with its thiol group serving as a ligand to Zn_1 and participating in a hydrogen bond to Ser102.

A short interaction between the thiol group of MMP and the Oγ oxygen of Ser102 makes an important contribution to the inhibitor potency of this phosphonate

The interaction between the thiol of MMP and the Oγ oxygen of Ser102 is too short to be a standard hydrogen bond and too long to be a covalent bond. The O$\gamma\cdots$S distances are 2.65 and 2.75 Å for the A and B sites, respectively. These distances are much shorter than the combined van der Waals radii of O and S (3.2 Å) even if the estimated errors for the S$\cdots$Oγ bond length (0.05 Å/0.06 Å in the A/B sites) are taken into account. Reported S-H$\cdots$O hydrogen bond distances in crystal structures range from 3.3–3.6 Å (Desiraju & Steiner, 1999). Structural studies provide examples of O$\cdots$O and N$\cdots$O hydrogen bonds having distances less than 2.5 Å (Gerlt & Gassman, 1993; Usher et al., 1994; Carlow et al., 1995). This distance is 0.25–0.35 Å shorter than the typical O$\cdots$O and N$\cdots$O hydrogen bonds centered around 2.75–2.85 Å (Desiraju, 1991) and 0.3–0.5 Å shorter than the van der Waals contact distances. These interactions have been classified as low barrier hydrogen bonds (LBHB) (Cleland & Kreevoy, 1994; Frey et al., 1994; Shan et al., 1996). The assignment of LBHBs is typically based on the heteroatom distance from X-ray crystallography and/or the observation of a highly deshielded proton in ^{1}H NMR spectroscopy (16–20 ppm). These hydrogen bonds can supply up to 10–20 kcal/mol binding energy. They are often invoked to explain the enzymatic deprotonation of carbon acids in enzyme systems (Gerlt & Gassman, 1993). Several X-ray crystal structures of enzyme complexes with transition state analogs have offered examples of LBHBs suggesting the involvement of the LBHB in transition state stabilization (Usher et al., 1994; Carlow et al., 1995). In the AP-MMP complex, the average O$\gamma\cdots$S distances in the A and B sites is 2.70 Å, 0.50 Å shorter than the van der Waals contact distance. Thus, the interaction between the thiol group of MMP and the side chain of Ser102 may represent a novel LBHB existing between a sulfur and an oxygen atom. Bond strength can be correlated with the distance between the participating heteroatoms. Thus, the strength of the O$\gamma\cdots$S bond may partly contribute to the greater inhibitory potency of MMP compared to PAA.

The crystal structures of the AP-MMP complex and the AP-PAA complex provide a useful framework for evaluating the potency of similar types of AP inhibitors

One of the most puzzling aspects of alkaline phosphatase inhibition is its dependence on inhibitor length. For example, mercaptoethylphosphonic acid is a substantially better inhibitor than MMP, and mercaptopropylphosphonic acid is even better (Myers et al., 1997). In addition, phosphonopropionic acid is a better inhibitor than PAA (Myers et al., 1997). Clearly, longer inhibitors show higher inhibitory potency within a family of similar functionality. Consideration of the two AP-inhibitor structures suggests a reason for this trend.

The interaction between Zn_1 and the carboxyl oxygen of PAA is fairly long with distances of 3.2 Å in the A site and 3.6 Å in the B site. Since these distances are rather long, the carboxylate group cannot be considered a direct ligand to Zn_1. However, electrostatic interactions operate over longer distances, so the interaction between Zn_1 and the carboxylate of PAA may offer some stabilization. The pendant carboxylate of PAA may participate in a long-range electrostatic interaction with Zn_1 while the phosphonate group maintains contact with Zn_2 and the active site Arg166. Phosphonopropionic acid is a longer molecule and can probably accommodate this reach somewhat better than PAA. MMP, however, is too short to make the multiple point contacts of PAA. Instead, MMP forms a strong contact to Zn_1 of the enzyme through its thiol group leaving the phosphonate unliganded. The longer versions of this molecule, such as mercaptoethylphosphonic acid and mercaptopropylphosphonic acid, may make additional contacts with the Zn_1 cofactor of the enzyme through the phosphonate group and are therefore better binding inhibitors. Unfortunately, attempts to obtain crystals of the AP-mercaptoethylphosphonic acid complex suitable for structural analysis have not been successful. Based on the present study of the AP complexes with PAA and MMP, however, the inhibitor length of the phosphonate may provide more opportunities for enzyme-inhibitor interactions overcoming the limitation imposed by the shallow active site pocket.

The enzyme-inhibitor complexes in the AP-PAA and AP-MMP structures can also explain the general inadequacy of phosphonates as inhibitors of AP

The substitution of the bridging oxygen of the substrate with a methylene group of a phosphonate results in a significant size change. This substitution reduces phosphonate binding 10–1,000-fold compared to the substrate (K_M = 10 μM) and results in a rather confined fit in the active site pocket as inferred from the X-ray crystal structures of the AP-inhibitor complexes. The bridging methylene carbon of PAA and MMP is roughly equidistant between a guanidinium nitrogen (η1) of Arg166 and the imidazole ring carbon (Cϵ) of His412. In both enzyme-inhibitor complexes, the average heavy atom distance between the methylene carbon and the η1 nitrogen of Arg166 is 2.8 Å. The average heavy atom distance between the methylene carbon and the Cϵ carbon of His412 is 3.2 Å in both structures. With the inclusion of estimated atomic errors (Table 2), these distances fall at the short end limit. For example, 3.5 Å is the lower limit for C$\cdots$C interactions while 3.0 Å is usually the lower limit for weak C$\cdots$O interactions (Desiraju & Steiner, 1999).

While the resolution problem complicates the interpretation of the interatomic contact distances, the active site pocket probably cannot accommodate groups much larger than a methylene carbon at the bridging position. Difluorophosphonates, for example, are very poor inhibitors of the enzyme. Some of the steric collisions occurring between an unsubstituted carbon at the bridging position and the enzyme may be minimized by the hybridization of the atom. For example, vinyl phosphinic acid (VPA) binds 20 times

more tightly than PAA and twice more tightly than MMP (K.M. Holtz, unpubl. obs.) without any additional functional groups. Based on the structural study, the general ineffectiveness of phosphonates as inhibitors of AP probably derives from both steric collisions within the small active site pocket as well as the electronegativity difference of the oxygen to methylene substitution. These obstacles to inhibition may be overcome with the addition of pendant groups capable of metal ligation.

The close enzyme-inhibitor distances may represent forced contacts determined by stronger electrostatic interactions

The close contacts involving the methylene groups of the inhibitors are determined by the formation of a network of strong, dominating hydrogen bonds and salt bridges between the inhibitors and the active site. For example, the thiol group of MMP in the AP-MMP complex forms electrostatic interactions to Zn_2 and the Oγ of Ser102. Similarly, the phosphinyl oxygens of PAA interact with the zinc ions and Arg166 in the AP-PAA complex. The pattern of close contacts observed between the methylene carbon of the inhibitors and the enzyme probably represent steric collisions and unfavorable crowding that is tolerable due to the strength of these other interactions. The fact that the crystallized enzyme associates with the inhibitor with soaking, however, suggests that the contacts involving the methylene carbon are not sufficiently destabilizing to preclude binding.

While the methylene carbon is involved in three close contacts with the enzyme, at least one has the geometrical and chemical potential to form a weak, stabilizing C-H···N hydrogen bond

Even though dictated by electrostatic interactions, the close contact between the guanidino nitrogen (η_1) of Arg166 and the methylene carbon of the inhibitors has the geometrical potential to form a stabilizing, nonconventional C-H···N hydrogen bond. The relevance of C-H···O/N hydrogen bonds in small molecules and biological structures has recently gained acceptance and recognition (Taylor & Kennard, 1982; Desiraju, 1991; Wiberg et al., 1991; Steiner & Saenger, 1993; Desiraju & Steiner, 1999). The geometrical properties of these hydrogen bonds have been characterized from neutron and X-ray diffraction structures (Desiraju & Steiner, 1999). Accordingly, C-H···N bonds are slightly longer than C-H···O bonds that have distances of 3.0–4.0 Å. Despite the use of refinement restraints, the bond lengths for the C···N interactions in the AP-PAA and AP-MMP complexes lie at the short end limit when coordinate errors are applied (Table 2). The larger uncertainties associated with the complexes at the resolution of the structure determinations may also contribute to the shorter values for the heavy atom distances. Furthermore, the extreme limits are not well defined for these types of hydrogen bonds, and due to their weakness they are easily distorted by local environment and crystal packing forces (Desiraju & Steiner, 1999). Consequently, the bond lengths and angles vary over a wider range than the conventional hydrogen bond. Despite the short contact distances, the calculated bond angles for the AP-PAA (144°) and AP-MMP (151°) complexes after normalizing the geometry are not highly bent and are close to the average bond angle of 150° for a strong C-H···O bond (Desiraju & Steiner, 1999).

To have the chemical potential to form the C-H···N hydrogen bond, the side chain of Arg166 must be deprotonated and the methylene proton of the inhibitor must be sufficiently acidic

Evidence indicates that the active site of AP significantly lowers the pK_a value of the amino group of Arg166, allowing the deprotonated side chain to function as proton acceptor. The commonly accepted pK_a value for the guanidino amino group of Arg166 is 12–13, however, the positively charged active site of AP (three divalent cations) lowers this value to around 7–8. Intrinsic pK_a values have been calculated for the active site Arg166 using the method of Honig as implemented in the program DELPHI (Soman et al., 1989). The results indicate that the pK_a of Arg166 is downshifted by 4.6 units in the presence of the inhibitor and 4.9 U in its absence. pK_a perturbations of this magnitude in the active sites of phosphatases and other enzymes have precedence (Zhang & Dixon, 1994). The side chain of Arg166 can serve as a proton acceptor and engage in a hydrogen bond with an activated methylene group of the inhibitors.

The methylene carbon of the inhibitors may be activated for proton donation due to electrostatic stabilization in the active site of AP. pK_a depressions for carbon acids in the active sites of enzymes are well documented (Gerlt & Gassman, 1993). The enzymatic racemizations of fumarase, citrate synthase, aconitase, and mandelate racemase involve abstraction of an α-proton adjacent to a carboxylate group. The tautomerization reactions of triose phosphate isomerase and enolase remove protons from carbons adjacent to phosphate dianions and carboxylate groups. Electrostatic stabilization and neutralization of the carboxylate and/or phosphate groups are achieved through metal ions and/or cationic side chains in all the above-mentioned enzymes (Flint et al., 1992; Kennedy & Stout, 1992; Gerlt & Gassman, 1993; Flint, 1994; Zhang et al., 1997). Metal and side-chain coordination of the above substrates can sufficiently lower the pK_a of the α-proton by 10 units or more. In an analogous manner, the pK_a for the methylene group of MMP and PAA can be lowered by active site coordination of the adjacent functional groups to the metal ions and/or Arg166. In the AP-PAA complex, the phosphinyl group of PAA is neutralized by interactions with Zn_1, Zn_2, and Arg166. The long interaction between the carboxylate and Zn_1 also may offer some charge neutralization. In MMP, the thiol group is neutralized by interactions to Zn_2 and the Oγ oxygen atom of Ser102. The binding modes of PAA and MMP in the active site of AP form an electron sink at the methylene carbon increasing the acidity of the relatively nonacidic α-proton of the inhibitor molecules. The active site induced pK_a shifts may allow the methylene group to donate a proton to the neutral amino group of Arg166.

Inhibition studies with a mutant AP enzyme do suggest that the interaction between Arg166 and the methylene carbon is weakly stabilizing. In the AP-MMP complex, the inhibitor makes only one close contact to the guanidinium group of Arg166 through the methylene carbon. In the R166A mutant AP, arginine at position 166 is replaced with an alanine removing the possibility of a C-H···N hydrogen bond. The K_i value for MMP inhibition of this mutant is ~2.5-fold larger. This reduction in MMP inhibition corresponds to approximately −0.5 kcal/mol stabilization energy. Energies for the weakest C-H···O/N interactions are estimated around −0.5 kcal/mol; however, the energy of van der Waals interactions is also around this value (Desiraju & Steiner, 1999). The results suggest that Arg166 does make a rather small contri-

bution to inhibitor stabilization. Whether this contribution is due to an unconventional C-H···N hydrogen bond or van der Waals interactions cannot be definitively established from this study.

Summary

The X-ray crystal structures of the AP-PAA and the AP-MMP complexes provide valuable information on alkaline phosphatase inhibition. The pattern of close contacts observed between the inhibitors and the active site of the enzyme may be due to crystal packing forces and a rather small binding pocket in AP. Of these close contacts, one has the potential to offer stabilization as a C-H···N hydrogen bond.

Materials and methods

Materials

Agar, agarose, ampicillin, *p*-nitrophenylphosphate, magnesium chloride, and zinc chloride were purchased from Sigma Chemical Co. (St. Louis, Missouri). Phosphonoacetic acid was purchased from Aldrich Chemical Co. (Milwaukee, Wisconsin). Mercaptomethylphosphonic acid was synthesized according to standard procedures (Myers et al., 1997). Tris, sucrose, and enzyme-grade ammonium sulfate were supplied by ICN Biomedicals (Costa Mesa, California). Tryptone and yeast extract were obtained from Difco Laboratories (Detroit, Michigan).

Enzyme preparations

E. coli alkaline phosphatase was isolated as previously described (Chaidaroglou et al., 1988). *E. coli* SM547 cells transformed with the plasmid pEK48 was used as the host strain for expression of wild-type alkaline phosphatase. The concentration of purified enzyme was determined from absorbance measurements at 280 nm using an extinction coefficient of 0.71 $cm^2\ mg^{-1}$ (Plocke & Vallee, 1962).

Enzyme assays

Alkaline phosphatase activity in the presence and absence of inhibitor was measured spectrophotometrically using *p*-nitrophenyl phosphate as the substrate (Garen & Leventhal, 1960). The release of the *p*-nitrophenolate chromophore was monitored at 410 nm. Assays were performed on a Beckman DU-64 spectrophotometer. Temperature was regulated at 25.0 ± 0.5 °C using a circulating constant-temperature bath. The buffer system was 1.0 M Tris pH 8.0. Stock solutions of PAA (1.0 M) and MMP (0.1 M) were prepared in deionized water. K_i values for PAA and MMP were determined from double-reciprocal plots of the data.

Crystallization and inhibitor soaking

Wild-type alkaline phosphatase was crystallized by vapor diffusion using hanging drops of 15 μL. The enzyme solution, at ~30 mg/mL, was first dialyzed against a 20% saturated solution of $(NH_4)_2SO_4$ in 100 mM Tris, 10 mM $MgCl_2$, 0.01 mM $ZnCl_2$ (pH 9.5). Crystals formed in reservoirs with the ammonium sulfate concentration between 39 and 43% saturated. Crystals were transferred into stabilizing solution containing 55% saturated $(NH_4)_2SO_4$, 100 mM Tris, 10 mM $MgCl_2$, 1 mM $ZnCl_2$ at pH 7.5.[4] Crystals were gradually introduced to the inhibitors by soaking in stabilization solution containing inhibitor. The concentration of inhibitor in the above stabilizing solution was increased in increments. Before mounting in glass capillaries, individual crystals of alkaline phosphatase were soaked at levels of 10 mM PAA and 100 μM MMP.[5]

X-ray data collection

The diffraction data were collected using two area detectors (Area Detector Systems, San Diego, California), driven by a VAX ALPHA 3300 computer and linked to Rigaku RU-200 rotating-anode generator operated at 50 kV and 150 mA using the Crystallographic Facility in the Chemistry Department of Boston College. Diffraction data for the AP-PAA and AP-MMP complexes were collected to 2.20 and 2.00 Å, respectively. For both structural complexes, the data collection statistics are summarized in Table 3. For the structure of the AP-PAA complex, a total of 59,057 unique reflections were obtained from measurements with an average redundancy of 3.1 (Table 3). For the structure of the AP-MMP complex, a total of 78,354 unique reflections were obtained from measurements with an average redundancy of 2.6 (Table 3).

Merging of the reflections was accomplished using the software provided by Area Detector Systems. After correction for Lorentz and polarization effects, a scale factor was calculated for multiple measurements and symmetry-related reflections.

Modeling and structural refinement

The coordinates were refined for each inhibitor complex using the wild-type coordinates for *E. coli* alkaline phosphatase as the initial model, with inorganic phosphate and the inhibitor molecule removed. X-PLOR V. 3.1 (Brünger, 1992) and IMPLOR (Polyvision, Inc., Hopedale, Massachusetts) were used to refine the coordinates. SHELXL-97 (Sheldrick & Schneider, 1997) was used in the final refinement cycles. Initial electron density ($2F_o - F_c$) and ($F_o - F_c$) maps were calculated. In both cases, the difference Fourier maps clearly showed extraneous electron density in the active site corresponding to the inhibitors. The initial ($F_o - F_c$) maps were used to model in structures of the inhibitors. For the AP-MMP structure, the inhibitor molecule was modeled in two possible orientations, i.e., one with the phosphonate directed into the active site and the other with the thiol group directed into the active site coordinated to Zn_1. The inhibitor structures of PAA and MMP were constructed in QUANTA (BioSym/MSI, San Diego, California) and energy minimized using the force field CHARMm (Brooks et al., 1983). Water ligands to the metal ions were also included in the second round of refinement. The enzyme-inhibitor structures were further refined by positional refinement, temperature factor refinement, and simulated annealing. Positional and temperature factor refinement improved working and free *R*-factors initially. The refinements were carried out using Silicon Graphics Indigo II computers. An automated water placement feature of IMPLOR was used to add solvent water molecules based on the difference Fourier map ($F_o - F_c$), their distance from surrounding

[4] Crystals obtained at pH 9.5 are stabilized at pH 7.5 to ensure full occupancy of Zn and Mg at the metal sites.

[5] The AP crystal for mercaptomethylphosphonate was soaked at a level of the inhibitor that was six times lower than the K_i value. Significant deterioration of the crystal was observed after soaking at 100 μM for 6 h.

Table 3. *Data collection summary of the AP-PAA and AP-MMP complexes*

Inhibitor complex	AP-PAA	AP-MMP
Space group	I222	I222
d_{min} (Å)	2.2	2.0
Reflections		
Total	180,502	202,714
Unique	59,057	78,354
Completeness (%)	92.6	92.6
Last shell	79.6 (2.20–2.40 Å)	72.6 (2.00–2.15 Å)
$I/\sigma(I)$	6.6	7.2
Last shell	1.2 (2.20–2.40 Å)	1.3 (2.00–2.15 Å)
Average redundancy	3.1	2.6
Last shell	2.0 (2.20–2.40 Å)	1.7 (2.00–2.15 Å)
Unit cell (Å)	$a = 194.77$	$a = 194.83$
	$b = 167.19$	$b = 167.10$
	$c = 76.59$	$c = 76.67$
Final R_{merge}[a]	0.078	0.052

[a] $$R_{merge} = \frac{\sum_{hkl}\sum_{i}|I_{mean} - I_i|}{\sum_{hkl}\sum_{i} I_i}.$$

residues, and their temperature factors. Full matrix refinement in SHELXL-97 (Sheldrick & Schneider, 1997) was used in the final stages to provide reliable estimates of the coordinate errors for distances in the AP-inhibitor complexes. The final coordinates have been deposited in the Protein Data Bank (AP-PAA, IEW8; AP-MMP, 1EW9).

Intrinsic pK_a calculation for Arg166

The method implemented by Soman et al. (1989) using the program DELPHI 3.0 (Sharp & Honig, 1990) was used to determine the change in intrinsic pK_a for the arginine residue found at position 166 in the active site of AP. The program calculates the electrostatic potential in and around the protein using a finite difference approximation to solve the nonlinear Poisson–Boltzmann equation. The program takes into account the difference in dielectric between the interior and exterior of the protein. The change in pK_a in the protein relative to the pK_a of the isolated amino acid in solution is given by $\Delta pK_a = \Delta\Delta G^\circ$ (elec)/1.4 (kcal), where $\Delta\Delta G^\circ$ (elec) is the difference in the total electrostatic energy of the amino acid in the two environments (Soman et al., 1989). The total electrostatic energy is calculated in DELPHI by using the following approximation

$$\Delta\Delta G^\circ(\text{elec}) = \Delta\Delta G_{\text{solv}} + \Delta G_{\text{dip}} + \Delta G_{\text{charge}}$$

which accounts for changes in solvation energy and for interactions of the charged residue with partial and permanent charges on the protein (Soman et al., 1989). Energy calculations in DELPHI (Sharp & Honig, 1990) were calculated using standard atomic radii for the atoms and using CHARMm (Brooks et al., 1983) charges for the polarizable groups. An internal dielectric of 2 and a solvent dielectric of 80 was assumed. The intrinsic change in pK_a for an arginine residue at position 166 was calculated in the presence and absence of bound PAA. An apparent charge of -2 was assumed for the inhibitor (i.e., the deprotonated form of the compound).

Acknowledgments

This work was supported by Grants GM42833 (to E.R.K.) and CA71736 (to T.S.W.) from the National Institutes of Health.

References

Bartlett PA, Hanson JE, Giannousis PP. 1990. Potent inhibition of pepsin and penicillopepsin by phosphorus-containing peptide analogues. *J Org Chem 55*:6268–6274.

Brooks BR, Bruccoleri RE, Olafson BD, States DJ, Swaminathan S, Karplus M. 1983. CHARMM: A program for macromolecular energy, minimization, and dynamics calculations. *J Comp Chem 4*:187–217.

Brünger AT. 1992. *X-PLOR, version 3.1*. New Haven, CT: Yale University Press.

Carlow DC, Smith AA, Yang CC, Short SA, Wolfenden R. 1995. Major contribution of a carboxymethyl group to transition-state stabilization by cytidine deaminase: Mutation and rescue. *Biochemistry 34*:4220–4224.

Chaidaroglou A, Brezinski DJ, Middleton SA, Kantrowitz ER. 1988. Function of arginine-166 in the active site of *Escherichia coli* alkaline phosphatase. *Biochemistry 27*:8338–8343.

Chakrabarti P. 1989. Geometry of interaction of metal ions with sulfur-containing ligands in protein structures. *Biochemistry 28*:6081–6085.

Cleland WW, Kreevoy MM. 1994. Low-barrier hydrogen bonds and enzymatic catalysis. *Science 264*:1887–1890.

Coleman JE. 1992. Structure and mechanism of alkaline phosphatase. *Annu Rev Biophys Biomol Struct 21*:441–483.

Desiraju GR. 1991. The C-H···O hydrogen bond in crystals: What is it? *Acc Chem Res 24*:290–296.

Desiraju GR, Steiner T. 1999. *The weak hydrogen bond: In structural chemistry and biology*. New York: Oxford University Press Inc.

Engel R. 1977. Phosphonates as analogues of natural phosphates. *Chem Rev 77*:349–367.

Flint DH. 1994. Initial kinetic and mechanistic characterization of *Escherichia coli* fumarase A. *Arch Biochem Biophys 311*:509–516.

Flint DH, Emptage MH, Guest JR. 1992. Fumarase A from *Escherichia coli*: Purification and characterization as an iron-sulfur cluster containing enzyme. *Biochemistry 31*:10331–10337.

Frey PA, Whitt SA, Tobin JB. 1994. A low-barrier hydrogen bond in the catalytic triad of serine proteases. *Science 264*:1927–1930.

Garen A, Leventhal C. 1960. A fine-structure genetic and chemical study of the enzyme alkaline phosphatase of *E. coli*. I. Purification and characterization of alkaline phosphatase. *Biochim Biophys Acta 38*:470–483.

Gerlt JA, Gassman PG. 1993. Understanding the rates of certain enzyme-catalyzed reactions: Proton abstraction from carbon acids, acyl-transfer reactions, and displacement reactions of phosphodiesters. *Biochemistry 32*:11943–11956.

Holden HM, Tronrud DE, Monzingo AF, Weaver LH, Matthews BW. 1987. Slow- and fast-binding inhibitors of thermolysin display different modes of binding: Crystallographic analysis of extended phosphonamidate transition-state analogues. *Biochemistry 26*:8542–8553.

Holtz KM, Stec B, Kantrowitz ER. 1999. A model of the transition state in the alkaline phosphatase reaction. *J Biol Chem 274*:8351–8354.

Hough E, Hansen LK, Birknes B, Jynge K, Hansen S, Hordvik A, Little C, Dodson EJ, Derewenda Z. 1989. High resolution (1.5 Å) crystal structure of phospholipase C from *Bacillus cereus*. *Nature 338*:357–360.

Kennedy MC, Stout CD. 1992. Aconitase: An iron-sulfur enzyme. In: Cammack R et al., ed. *Advances in inorganic chemistry*. London: Academic Press Inc. pp 323–339.

Kim EE, Wyckoff HW. 1991. Reaction mechanism of alkaline phosphatase based on crystal structures. Two-metal ion catalysis. *J Mol Biol 218*:449–464.

Kim H, Lipscomb WN. 1990. Crystal structure of the complex of carboxypeptidase a with a strongly bound phosphonate in a new crystalline form: Comparison with structures of other complexes. *Biochemistry 29*:5546–5555.

Lejczak B, Kafarski P, Zygmunt J. 1989. Inhibition of aminopeptidases by aminophosphonates. *Biochemistry 28*:3549–3555.

Lopez V, Stevens T, Lindquist RN. 1976. Vanadium ion inhibition of alkaline phosphatase-catalyzed phosphate ester hydrolysis. *Arch Biochem Biophys 175*:31–38.

Morgan BP, Scholtz JM, Ballinger MD, Zipkin ID, Bartlett PA. 1991. Differential binding energy: A detailed evaluation of the influence of hydrogen-bonding and hydrophobic groups on the inhibition of thermolysin by phosphorus-containing inhibitors. *J Am Chem Soc 113*:297–307.

Murphy JE, Stec B, Ma L, Kantrowitz ER. 1997. Trapping and visualization of a covalent enzyme-phosphate intermediate. *Nat Struct Biol 4*:618–622.

Myers JK, Antonelli SM, Widlanski TS. 1997. Motifs for metallophosphatase inhibition. *J Am Chem Soc 119*:3163–3164.

Ohlsson JT, Wilson IB. 1974. The inhibition of alkaline phosphatase by periodate and permanganate. *Biochim Biophys Acta 350*:48–53.

Plocke DJ, Vallee BL. 1962. Interaction of alkaline phosphatase of *E. coli* with metal ions and chelating agents. *Biochemistry 1*:1039–1043.

Reid TW, Wilson IB. 1971. *E. coli*. alkaline phosphatase. In: Boyer PD, ed. *The enzymes*. New York: Academic Press. pp 373–415.

Shan S, Loh S, Herschlag D. 1996. The energetics of hydrogen bonds in model systems: Implications for enzymatic catalysis. *Science 272*:97–101.

Sharp K, Honig B. 1990. Electrostatic interactions in macromolecules: Theory and applications. *Annu Rev Biophys Chem 19*:301–332.

Sheldrick GM, Schneider TR. 1997. SHELXL: High-resolution refinement. *Methods Enzymol 277*:319–343.

Soman K, Yang AS, Honig B, Fletterick R. 1989. Electrical potentials in trypsin isozymes. *Biochemistry 28*:9918–9926.

Sowadski JM, Handschumacher MD, Murthy HM, Foster BA, Wyckoff HW. 1985. Refined structure of alkaline phosphatase from *Escherichia coli* at 2.8 Å resolution. *J Mol Biol 186*:417–433.

Sowadski JM, Handschumacher MD, Murthy HM, Kundrot CE, Wyckoff HW. 1983. Crystallographic observations of the metal ion triple in the active site region of alkaline phosphatase. *J Mol Biol 170*:575–581.

Steiner T, Saenger W. 1993. Role of C-H···O hydrogen bonds in the coordination of water molecules. Analysis of neutron diffraction data. *J Am Chem Soc 115*:4540–4547.

Taylor R, Kennard O. 1982. Crystallographic evidence for the existence of C-H···O, C-H···N, and C-H···Cl hydrogen bonds. *J Am Chem Soc 104*:5063–5070.

Usher KC, Remington SJ, Martin DP, Drueckhammer DG. 1994. A very short hydrogen bond provides only moderate stabilization of an enzyme-inhibitor complex of citrate synthase. *Biochemistry 33*:7753–7759.

Volbeda A, Lahm A, Sakiyama F, Suck D. 1991. Crystal structure of *Penicillium citrinum* P1 nuclease at 2.8 Å resolution. *EMBO J 10*:1607–1618.

Wiberg KB, Waldron RF, Schulte G, Saunders M. 1991. Lactones. 1. X-ray crystallographic studies of nonanolactone and tridecanolactone: Nature of CH···O nonbonded interactions. *J Am Chem Soc 113*:971–977.

Zhang E, Brewer JM, Minor W, Carreira LA, Lebioda L. 1997. Mechanism of enolase: The crystal structure of asymmetric dimer enolase—2-phospho-D-glycerate/enolase—phosphoenolpyruvate at 2.0 Å resolution. *Biochemistry 36*:12526–12534.

Zhang ZY, Dixon JE. 1994. Protein tyrosine phosphatases: Mechanism of catalysis and substrate specificity. *Adv Enzymol Relat Areas Mol Biol 68*:1–36.